Journal of Materials Chemistry A

ROYAL SOCIETY OF CHEMISTRY

PAPER

View Article Online
View Journal | View Issue

Cite this: J. Mater. Chem. A, 2026, 14, 14544

Highly flexible, strong and dynamic recovery solid-solid phase change materials based on polythiourethane–polyurethane for thermal management

Xiaohua Liu,†[a] Hongfei He,†[a] Hongliang Ding,[a] Chuanshen Wang,[a] Lu Liu,[b] Na Sun,*[a] Keqing Zhou,[c] Wei Yang,[d] Jixin Zhu[a] and Bin Yu*[a]

Addressing the critical challenges of leakage in physically encapsulated phase change materials (PCMs) and the non-recyclability of chemically crosslinked PCMs, this study introduces a sustainable PCM system based on dynamically reversible thiocarbamate bonds (TCBs). The TCB-crosslinked network enables exceptional shape stability (zero leakage observed) during phase transitions and endows the material with efficient recyclability. By modulating polyethylene glycol (PEG) weight content, the phase transition temperature is precisely tunable within a broad range (15.2–51.5 °C), ensuring adaptability to diverse thermal management scenarios. The material exhibits a high latent heat capacity of 77.0 J g^{-1}, supported by a microphase-separated structure and multiple hydrogen-bonding networks that enhance thermal reliability. Remarkably, a synergistic balance between crosslinking density and dynamic bonds confers outstanding mechanical properties, achieving a tensile strength of 28.3 MPa and ductility of 976.0%, overcoming the brittleness typical of conventional PCMs. Leveraging the dynamic reversibility of TCBs, solvent-mediated decrosslinking and hot-press molding methods enable material recovery rates exceeding 90%, establishing a closed-loop lifecycle. This work provides a paradigm-shifting strategy for designing high-performance, recyclable PCMs that integrate robust thermal regulation, structural integrity, and environmental sustainability for advanced thermal energy storage applications.

Received 25th December 2025
Accepted 27th February 2026

DOI: 10.1039/d5ta10488b

rsc.li/materials-a

Introduction

In recent years, escalating environmental challenges and a growing emphasis on sustainability have accelerated the development of advanced energy utilization technologies.[1–5] Within this context, thermal energy, a fundamental and critical energy form, plays a pivotal role across diverse industrial and domestic applications. However, the efficient storage and utilization of thermal energy continue to face significant obstacles, including energy dissipation and limitations in applicability.[6]

Phase Change Materials (PCMs), recognized for their high energy storage density and operational stability, have emerged as promising candidates to address these challenges. They have garnered substantial attention in fields such as Thermal Energy Storage (TES), thermal management of electronic devices, and infrared stealth applications.[7–9] PCMs operate based on latent heat absorption/release during phase transitions, which commonly include solid–liquid, liquid–gas, solid–gas, and solid–solid transformations.[10] While solid–liquid and liquid–gas systems often exhibit higher enthalpy values,[10] they are plagued by significant leakage risks associated with the storage of liquid or gaseous phases.[11–14] This inherent limitation compromises their long-term practicality and reliability.

Solid–Solid Phase Change Materials (SSPCMs) present a compelling alternative. SSPCMs maintain a nearly constant volume throughout their phase transitions, thereby eliminating the critical leakage issues inherent in other phase change systems and obviating the need for encapsulation or support materials.[15] This intrinsic characteristic significantly enhances their stability and reliability, positioning SSPCMs as a key technology for advanced thermal energy storage.[15] Furthermore, SSPCMs demonstrate remarkable tunability; by adjusting the relative content of phase change components, cross-linking agents, and other constituents, their phase transition

[a]State Key Laboratory of Fire Science, University of Science and Technology of China, 96 Jinzhai Road, Hefei, Anhui, 230026, China. E-mail: yubin@ustc.edu.cn; sunna@ustc.edu.cu

[b]College of Materials Science and Engineering, Chongqing University, 174 Shazhengjie, Shapingba, Chongqing, 400044, China

[c]Faculty of Engineering, China University of Geosciences (Wuhan), Wuhan, Hubei 430074, China

[d]School of Energy, Materials and Chemical Engineering, Hefei University, 99 Jinxiu Avenue, Hefei, Anhui 230601, PR China

† These authors contributed to this work equally.

temperature range can be precisely tailored to meet specific thermal management requirements.[16]

Polyethylene glycol (PEG) is a particularly promising component for SSPCMs due to its adjustable phase transition temperature and excellent thermal properties. Numerous studies have explored PEG-based form-stable PCMs (FSPCMs), often employing physical encapsulation strategies to achieve shape stability.[17–20] However, this approach frequently suffers from long-term stability issues, making leakage prevention challenging over extended periods.[20–22] Alternatively, chemically crosslinked structures offer another effective route for developing SSPCMs, integrating the phase change component into a stable polymer network.[23–25] While this enhances material integrity, conventional chemical crosslinking introduces significant drawbacks, notably reduced recyclability and potential enthalpy loss, highlighting the need for innovative strategies that reconcile performance with sustainability.

Consequently, incorporating dynamic covalent bonds into crosslinked networks has emerged as a promising strategy. Such bonds can enable recyclability and processability while maintaining mechanical strength. Various dynamic chemistries have been explored for SSPCM synthesis, including Diels–Alder reactions,[26] transesterification,[27–29] disulfide bond exchange,[30] dynamic Schiff base chemistry,[31–33] and supramolecular interactions like metal–ligand coordination.[34,35] Nevertheless, achieving effective recyclability often relies on specialized precursors requiring complex synthesis or highly reactive catalysts, which can lead to material degradation over time. Therefore, developing SSPCMs that combine high energy storage capacity, robust performance, simple synthesis, and cost-effectiveness using readily available materials remains a significant challenge.

Polythiourethane (PTU), characterized by thiocarbamate bonds (TCBs),[36] has found applications in diverse fields such as additive manufacturing,[37,38] biomedicine,[39] and fire warning systems.[40] Critically, TCBs exhibit intrinsic dynamic reversibility. In this study, we leverage this property to develop a novel SSPCM system. PEG serves as the phase change component for heat storage and release, while its inherent leakage tendency is mitigated through covalent integration into a PTU network formed *via* the reaction of PEG with isocyanate and a tetrafunctional thiol chain extender (PETMP). The resulting dynamically crosslinked network, facilitated by the reversible TCBs, is designed to provide exceptional shape stability during phase transitions, overcome the brittleness typical of conventional PCMs, and offer efficient recyclability through solvent-mediated decrosslinking or hot-pressing routes. This approach aims to deliver a high-performance, sustainable SSPCM integrating robust thermal regulation, structural integrity, and environmental sustainability.

Results and discussion

To systematically investigate the influence of PEG content on the physicochemical properties of PTUs, including mechanical behavior, crystallization characteristics, phase transition enthalpy, and leakage resistance, a series of PTU samples were synthesized by varying the molar ratio of PEG to PETMP. In this study, the PTU formulations are denoted as PETMP-*x*%, where *x* represents the molar fraction of PETMP employed in the reaction feed. This compositional variation enables fine-tuning of the crosslinking density and segmental dynamics within the polymer network, which in turn governs both macroscopic mechanical performance and thermoresponsive behavior. Specifically, increasing the PEG content is expected to enhance segmental flexibility and crystallinity, whereas higher PETMP content contributes to a denser crosslinked network, potentially improving thermal stability and shape retention under elevated temperatures. The masses of all reagents utilized in the synthesis of PTUs are detailed in Table S1 (SI).

The chemical structure of the synthesized PTUs is schematically illustrated in Fig. 1a. The PTUs were prepared *via* a two-step step-growth polymerization process involving PEG, IPDI, and PETMP. The initial step proceeds through the formation of isocyanate-terminated prepolymers, followed by a thiol–isocyanate click reaction, yielding a crosslinked polymer network with thiourethane linkages.

The binding energy of the four hydrogen bonds present in PTUs was calculated, as shown in Fig. 1b, revealing that the strength of hydrogen bonds of the same type was comparatively greater, as indicated by their higher absolute binding energy values. This suggests a preferential tendency for PTUs to form hydrogen bonds with similar counterparts, a characteristic that may play a facilitative role in promoting microphase separation within the material system.

Fig. 1c and d illustrate the electrostatic potential (ESP) distributions of IPDI when interacting with two distinct reactant dimers. Notably, a comparative analysis of the ESP maps reveals a discernible reduction in the positive electrostatic potential surrounding the thiocarbamate bond in contrast to the carbamate bond. This attenuation of positive potential suggests a diminished electrostatic attraction toward potential hydrogen bond acceptors, which in turn implies a weakening of the intermolecular hydrogen bonding capability. The observed decrease in hydrogen bond strength can be attributed to the altered electronic environment induced by the thiocarbonyl substitution, which modulates the local charge distribution and reduces the bond's polarity.

Whole atomic molecular dynamics (MD) simulations were used to elucidate the accumulation state of structures in PTUs. In the context of MD simulation, two simulation systems were created. These systems are placed within the simulation pool to replicate the equilibrium conformation of the actual polymer chain. As shown in Fig. 1e and f the average cohesion energies of PETMP-90% and PETMP-92.5% were calculated to be 101 and 92 kJ mol^{-1}, indicating that there were more pronounced intermolecular interactions in PETMP-92.5%. In addition, according to the calculation results, the number of hydrogen bonds in PETMP-90% and PETMP-92.5% is 560 and 364 (Fig. 1g).

To evaluate the shape memory behavior of the PTU system, a hexagonally patterned thin film was fabricated and subjected to thermo-mechanical deformation tests, as shown in Fig. 1h. At an elevated temperature of 60 °C, the PTU film demonstrates

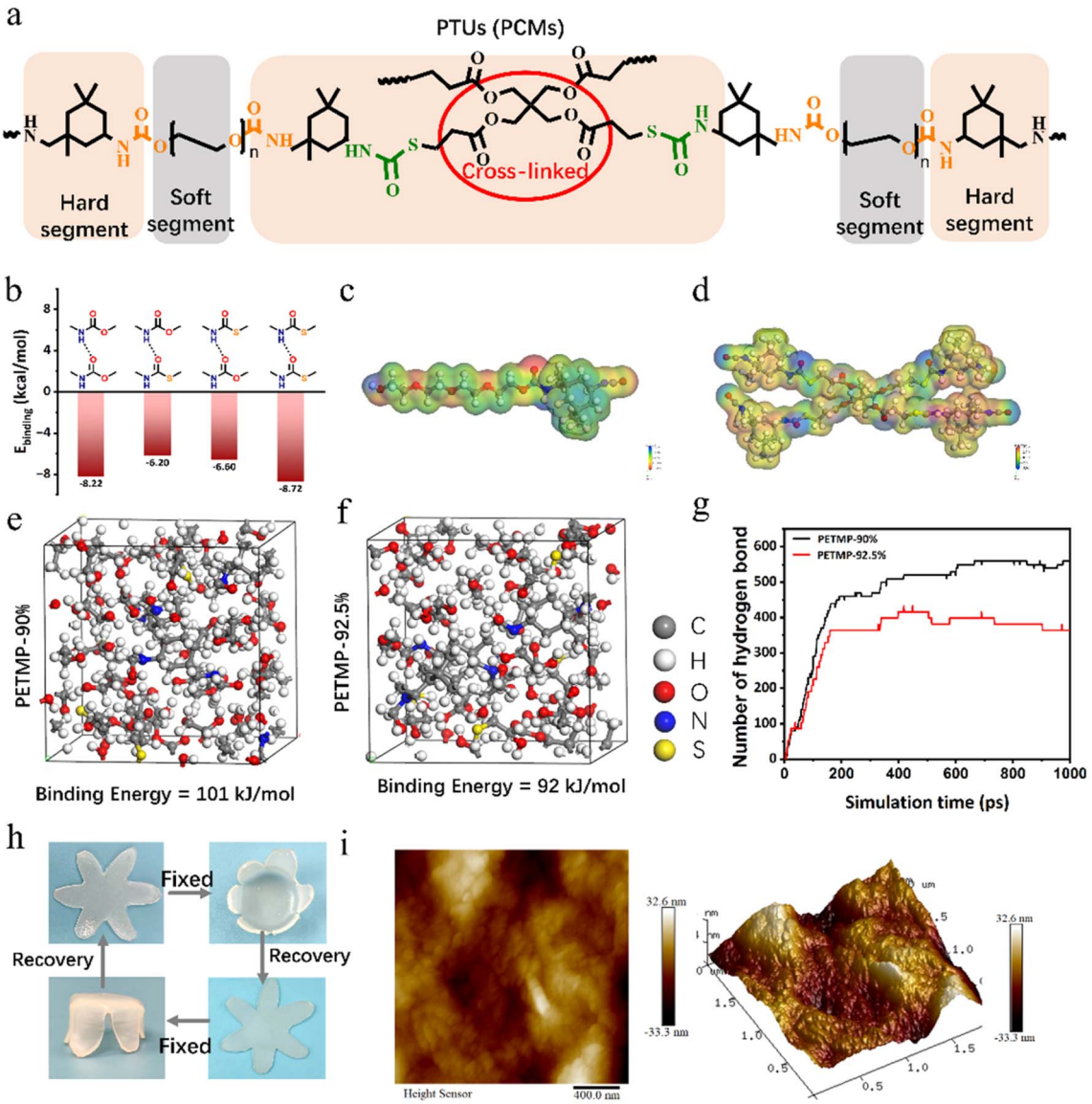

Fig. 1 (a) The structural formula; (b) four types of hydrogen bond binding energies. (c) Electrostatic potential of IPDI with PETMP dimer. (d) Electrostatic potential of IPDI with PEG dimer of PTUs (the red region corresponds to the electrophilic site, and the blue region corresponds to the nucleophilic site). MD snapshots for (e) PETMP-90% and (f) PETMP-92.5%. (g and h) Shape memory performance; (i) AFM testing.

high thermoplastic flexibility, allowing it to be bent freely to any desired angle. Upon cooling to ambient temperature, the deformed configuration is effectively retained, indicating a successful "fixing" of the temporary shape due to physical crosslinking and segmental motion restriction. Subsequently, reheating the film to 60 °C triggers the recovery process, wherein the polymer network progressively returns to its original undeformed geometry, as depicted in Fig. 1h. This thermally responsive shape memory behavior is attributed to the reversible soft segment mobility governed by temperature, coupled with the phase-separated morphology of PTU. The soft PEG domains enable temporary deformation under heating, while the hard domains provide a stable framework for shape fixation and recovery. This behavior underscores the potential of PTU materials for smart applications requiring reversible actuation or thermal programmability.

Fig. 1i presents the atomic force microscopy (AFM) image of the PTU film obtained at ambient temperature. The topographical contrast distinctly reveals two separate domains: the bright regions correspond to a soft, continuous phase, while the dark regions denote harder domains dispersed within the matrix. This pronounced morphological contrast indicates a clear microphase separation, likely originating from the intrinsic incompatibility between soft and hard segments in the segmented polymer structure. The accompanying surface roughness analysis further substantiates this phase-separated morphology. The height profile demonstrates the presence of surface protrusions with elevations reaching approximately 30 nm above the average plane. Despite these localized features,

the overall average surface roughness (R_a) of the film remains relatively low, measured at less than 10 nm (Fig. S3). This suggests that while microscale domain segregation is evident, the film maintains a generally smooth surface, which may be beneficial for optical clarity or interfacial adhesion in subsequent applications. Such hierarchical topographical features are characteristic of thermoplastic elastomers with well-defined phase structures and can significantly influence mechanical and surface–responsive properties.

The FT-IR spectra of the synthesized PTUs are presented in Fig. 2a. A prominent absorption peak at 1100 cm^{-1} is attributed to the symmetric stretching vibration of the C–O–C ether linkages originating from the PEG soft segments. Additionally, a broad absorption band centered around 3451 cm^{-1} corresponds to the N–H/O–H stretching vibration, indicative of hydrogen-bonding interactions within the polymer matrix. Multiple characteristic absorption peaks are observed at 2888, 1467, 961, and 841 cm^{-1}, which are associated with various C–H stretching and bending vibrations, reflecting the presence of

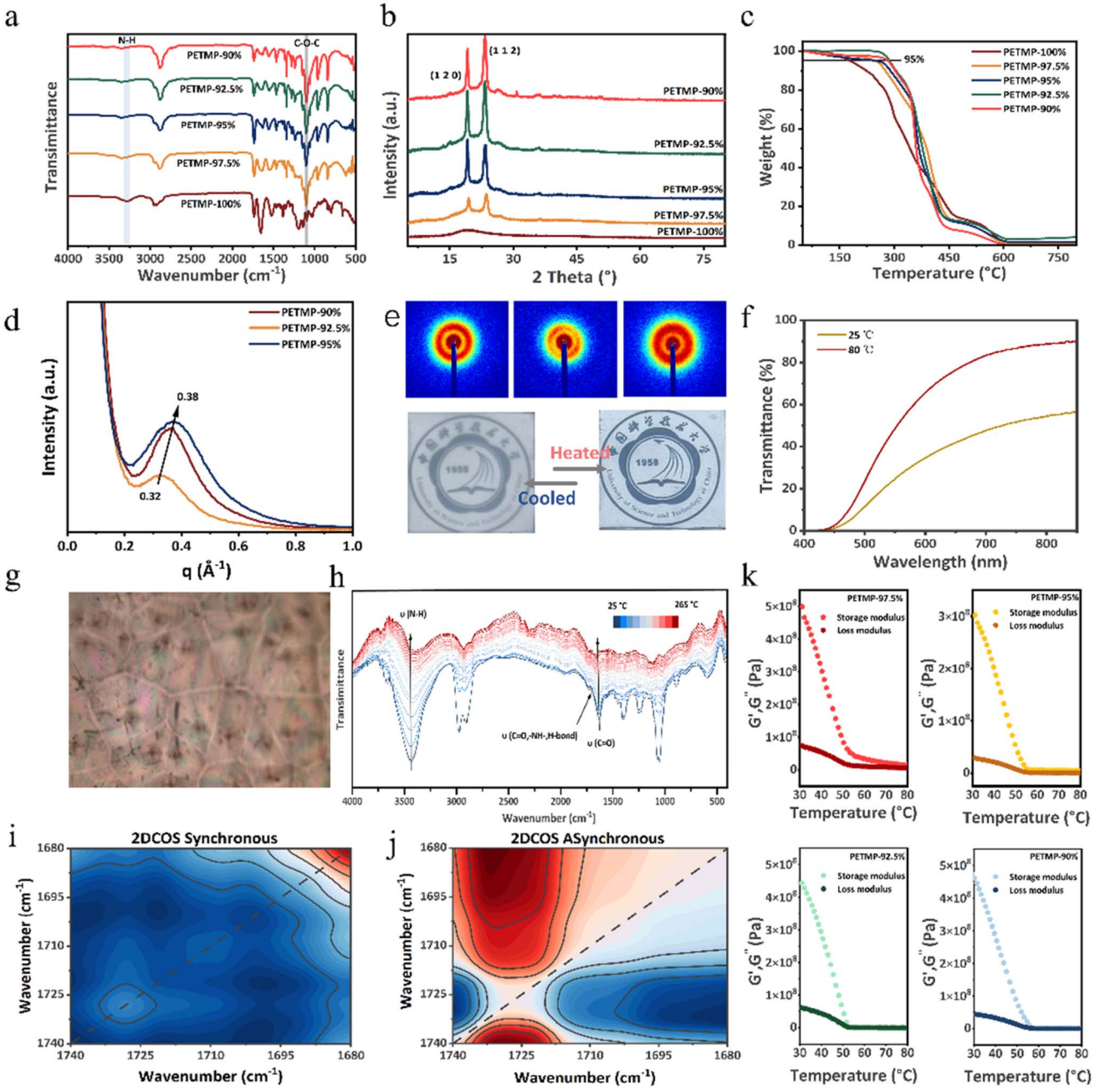

Fig. 2 (a) FT-IR, (b) XRD, (c) TGA (air); (d) one-dimensional SAXS curves; (e) digital photograph of transparency (at 25 °C and 80 °C) and SAXS diagram; (f) transmittance curves; (g) POM; (h) temperature-dependent FT-IR spectrum; (i and j) PETMP-90% two-dimensional spectra with temperature-dependent spectra; (k) DMA curves of PTUs.

aliphatic hydrocarbon chains and side groups. Compared with the spectrum of pristine PEG, the PTU spectrum shows a significant attenuation or disappearance of the absorption band at 2282 cm^{-1}, which is attributed to the stretching vibration of the isocyanate (–NCO) group of IPDI. This confirms the complete consumption of –NCO groups during the step-growth polymerization reaction. Moreover, the emergence of new absorption peaks at 1540, 1661, 1716, and 3331 cm^{-1} in the PTU spectrum is indicative of the successful formation of thiourethane linkages. Collectively, these spectral features substantiate the successful synthesis of PTU *via* the thiol–isocyanate click reaction and provide insight into the chemical structure and functional group transformations that occur during polymer formation. The disappearance of –NCO and the simultaneous emergence of urethane-specific peaks signify the completion of the reaction and the development of a highly crosslinked polymer network.

The crystalline characteristics of the synthesized PTUs directly govern their phase transition behavior, critically determining both the transition temperature and the magnitude of the latent heat. As corroborated by the X-ray diffraction (XRD) analysis presented in Fig. 2b, materials incorporating PEG-10k chains manifest distinct diffraction peaks at 2θ values of 19.5°, 23.7°, 26.6°, and 36.5°. These characteristic peaks align precisely with those observed in pristine PEG, corresponding to reflections from the (120), (112), (210), and (212) crystallographic planes, respectively. This compelling correspondence unequivocally demonstrates that the crystalline domains within the PTUs are predominantly orchestrated by the PEG segments. Consequently, the PTUs inherit the intrinsic crystal structure and exhibit favorable crystalline properties inherent to the PEG component. Furthermore, the XRD data reveal a pronounced positive correlation between PEG content within the PTU matrix and crystalline order. Specifically, the intensity of the characteristic PEG-associated diffraction peaks exhibits a systematic enhancement with increasing PEG concentration. This marked intensification signifies a progressive improvement in the overall crystallinity of the PTUs, ultimately culminating in superior crystallization performance for compositions richer in PEG. The enhancement in crystallinity is pivotal, as it directly underpins the efficacy of these materials as PCMs, influencing both energy storage capacity (latent heat) and the robustness of the phase transition.

Thermal stability constitutes a critical performance metric for PCMs, directly governing their operational lifespan and reliability in thermal energy storage systems. As quantitatively demonstrated by thermogravimetric analysis (TGA) and derivative thermogravimetry (DTG) profiles in Fig. 2c and S3, the synthesized PTUs exhibit exceptional thermal resilience across a composition-dependent gradient. The characteristic decomposition onset temperature ($T_{5\%}$), defined as the temperature at 5% mass loss, reveals a pronounced correlation with PETMP content (Table S3). This non-monotonic trend indicates that optimal crosslinking density exists. Such behavior originates from the competing effects of thiourethane bond density and PEG segment mobility. Remarkably, all formulations sustain operational integrity beyond 200 °C, with decomposition onsets exceeding industrial requirements for medium-temperature thermal storage (typically >180 °C). The simultaneous preservation of crystalline phase stability and thermal decomposition resistance confirms successful molecular design of PTUs as robust multifunctional PCMs.

The PTUs system constitutes a designer linear multiblock copolymer architecture, strategically engineered with alternating rigid hard segments derived from PETMP and flexible soft segment composed of PEG. The resulting nanoscale periodicity generates well-defined microphase-separated domains, a critical structural feature that governs both the mechanical integrity and phase-change functionality of these advanced materials. Quantitative analysis *via* synchrotron-based small-angle X-ray scattering (SAXS) reveals two fundamental characteristics of this self-assembled nanostructure (Fig. 2d). As the PETMP content decreases from 95% to 92.5% and further to 90%, the primary scattering vector (q) shifts from 0.38 $Å^{-1}$ to 0.32 $Å^{-1}$ and back to 0.38 $Å^{-1}$, respectively. Concurrently, the peak intensity transitions from strong to weak and back to strong. This non-monotonic behavior is attributed to the competing effects of microphase separation driven by the thermodynamic immiscibility between rigid PETMP and flexible PEG. At high PETMP content (95%), the dominant rigid segments form well-defined, densely packed microdomains with a characteristic spacing of $d = 2\pi/q \approx 16.5$ nm. The high peak intensity signifies strong electron density contrast and high coherence in the periodic nanostructure, consistent with pronounced microphase separation. Reducing PETMP to 92.5% dilutes the hard-segment matrix, leading to increased microdomain spacing ($d \approx 19.6$ nm) due to reduced spatial constraints on PEG chain aggregation. The weaker scattering peak indicates diminished long-range order and interfacial sharpness, likely caused by partial mixing or interfacial broadening between phases. Further decreasing PETMP to 90% enhances PEG crystallinity. The recovery of both q (0.38 $Å^{-1}$) and peak intensity suggests a transition to a PEG-dominated crystalline lattice with restored periodicity and interfacial contrast, where PEG crystallites dictate the nanostructure dimensions. Critically, the intensity minimum at PETMP-92.5% reflects a metastable state with compromised structural integrity, where insufficient hard-segment continuity coexists with incomplete PEG crystallization. This highlights the threshold-dependent nature of microphase separation in PTUs, wherein compositional tuning must balance segmental mobility and thermodynamic driving forces to optimize nanostructural order for functional performance.

The inherent biphasic nature of PEG comprising crystalline solid and homogeneous states—governs a striking optical transition in the derived PCMs. As systematically demonstrated in Fig. 2e, these PCMs exhibit fully reversible opacity-transparency switching across the phase transition temperature (T_g). In the crystalline phase at temperatures below T_g, light scattering at grain boundaries and crystalline–amorphous interfaces induces strong opacity due to refractive index mismatches. Upon heating above T_g, the collapse of crystalline domains triggers a solid-solid phase transition, resulting in a homogeneous isotropic melt with uniform refractive index

distribution. This structural homogenization eliminates scattering centers, thereby enabling near-complete optical transparency. By quantifying the change in transmittance of materials through ultraviolet-visible transmittance testing, the transmittance of PETMP-90% increased from about 55% at room temperature (25 °C) to about 89% at 80 °C (as shown in Fig. 2f).

The crystalline hierarchy of PTUs was systematically interrogated through polarized optical microscopy (POM) coupled with quantitative image analysis, revealing critical structure–property relationships governed by hard-soft segment interplay. As evidenced in Fig. 2g and S5, all PTU specimens exhibit characteristic Maltese cross-extinction patterns superimposed on radially symmetric spherulitic superstructures—a morphological fingerprint confirming epitaxial growth of PEG crystals within the thiourethane network matrix. Notably, the spherulite diameter demonstrates composition-dependent scaling, the spheroid size of PTUs is smaller than that of the original PEG. This size reduction originates from dual confinement mechanisms: (i) geometric restriction imposed by PETMP-derived nanodomains; (ii) dynamic suppression of PEG chain reptilation *via* hydrogen-bonding between TCBs and PEG ether oxygens in H-bonding.

The dynamic evolution of hydrogen-bonding networks in PETMP-90% was quantitatively resolved through temperature-dependent Fourier-transform infrared spectroscopy (FTIR), providing molecular insights into thermally triggered structural reorganization. As systematically tracked in Fig. 2h, three critical vibrational modes exhibit pronounced thermoresponsive behavior: (i) the intensity of free –NH– group peak ($\approx$1720 cm^{-1}) increases with temperature while the intensity of –NH– bending vibration peak ($\approx$1700 cm^{-1}) decreased, respectively, and (ii) the broad N–H stretching vibration centered at 3324 cm^{-1} (reflecting coupled thiourethane/urea N–H$\cdots$O=C interactions). During thermal ramping from 25 °C to 265 °C, these characteristic peaks undergo cooperative intensity attenuation accompanied by progressive blue shifts. Based on the temperature-dependent FT-IR results, 90% of the PETMP-2D correlated infrared spectra were acquired to reveal the specific temperature of the dissociation of multiple H-bonds (Fig. 2i and j). Two-dimensional spectra include synchronous and asynchronous correlation spectra. The pink area indicates the positive correlation strength area and the blue area indicates the negative correlated strength area.

Dynamic thermomechanical analysis (DMA) provides critical insights into the solid-state phase transition behavior of the synthesized PTU multiblock copolymers. As rigorously quantified in Fig. 2k under oscillatory shear at 1 Hz frequency, these materials exhibit distinctive viscoelastic signatures confirming a reversible solid-solid transition mechanism. Throughout the investigated temperature range (30–80 °C), the storage modulus (G') consistently dominates over the loss modulus (G''). This mechanical hierarchy unequivocally demonstrates perpetual elastic network percolation, stemming from dual structural constraints: (i) permanent chemical crosslinks formed by tetrafunctional PETMP nodes, and (ii) physical entanglements between semi-crystalline PEG domains. This phenomenon arises from the competitive interplay between chain mobility and network confinement: heating disrupts PEG crystallites, liberating constrained chains that undergo reptation through the thiourethane network meshes, thereby dissipating stored elastic energy through viscous flow. This thermorheological profile satisfies the critical criteria for solid-solid PCMs: melt confinement within crosslinked frameworks prevents macroscopic flow while enabling sub-T_g chain relaxations through free volume redistributions.

The molecular architecture–property relationships in PTU networks were rigorously elucidated through systematic modulation of two critical structural parameters: PEG soft segment molecular weight (M_n) and PETMP crosslinker density. As detailed in SI Tables S1 and S2, PTUs were synthesized with PEG M_n ranging from 4k to 10k Da while maintaining equivalent hydroxyl/thiol stoichiometry, and with PETMP molar fractions spanning 90% to 95% at fixed PEG M_n (10k). Uniaxial tensile analysis (Fig. 3a, b and S6) reveals profound mechanical tunability governed by chain topology: increasing PEG M_n from 4k to 10k enhances ultimate tensile strength from 23.0 $\pm$ 0.2 MPa to 28.3 $\pm$ 0.9 MPa and elevates elongation at break from 416.8 $\pm$ 154.4% to 877.3 $\pm$ 92.7% (Table S4). As demonstrated in Fig. 3c, PTU specimen weighing merely 40 mg sustains a 2.0 kg mass without fracture. Simultaneously, the film withstands 360° torsion without plastic deformation. The exceptional strength–toughness synergy in PTU originates fundamentally from a strain-induced crystallization (SIC) mechanism, wherein the microphase-separated architecture orchestrates a dynamic structural evolution under mechanical stimuli. The PTU matrix comprises nanoscale domains formed by the thermodynamic incompatibility between rigid PETMP blocks and flexible PEG segments. Upon deformation, these domains act as stress concentrators, triggering localized chain alignment of PEG soft segments along the strain axis. The reversible hydrogen bonds formed by thiocarbamate act as nodal entanglement, and the structure acts as a stress concentration point when stressed, induces a local high stress field, and drives the soft molecular chains to be arranged in a directional direction along the tensile direction, providing a topological basis for strain-induced crystallization. The soft segment (PEG) under low stress is in an unconventional grouping state. Under high strain, the molecular chain is highly oriented, and a temporary nanocrystalline region is formed by chain segment rearrangement. The crystallization process consumes a lot of energy, which significantly increases the fracture energy.

The viscoelastic relaxation behavior of PTU networks was investigated through temperature-dependent stress relaxation analysis. As depicted in Fig. 3e–g, the characteristic relaxation time exhibits an exponential reduction with increasing temperature for identical samples, consistent with thermally activated polymer dynamics. Concurrently, elevated PEG content accelerates stress decay at constant temperature, indicating enhanced chain mobility through plasticization effects. Quantitative analysis *via* Arrhenius formalism (Fig. 3h and Table S5) demonstrates that the apparent activation energy (E_a) increases systematically with higher PETMP content. This correlation arises from increased TCB density within the

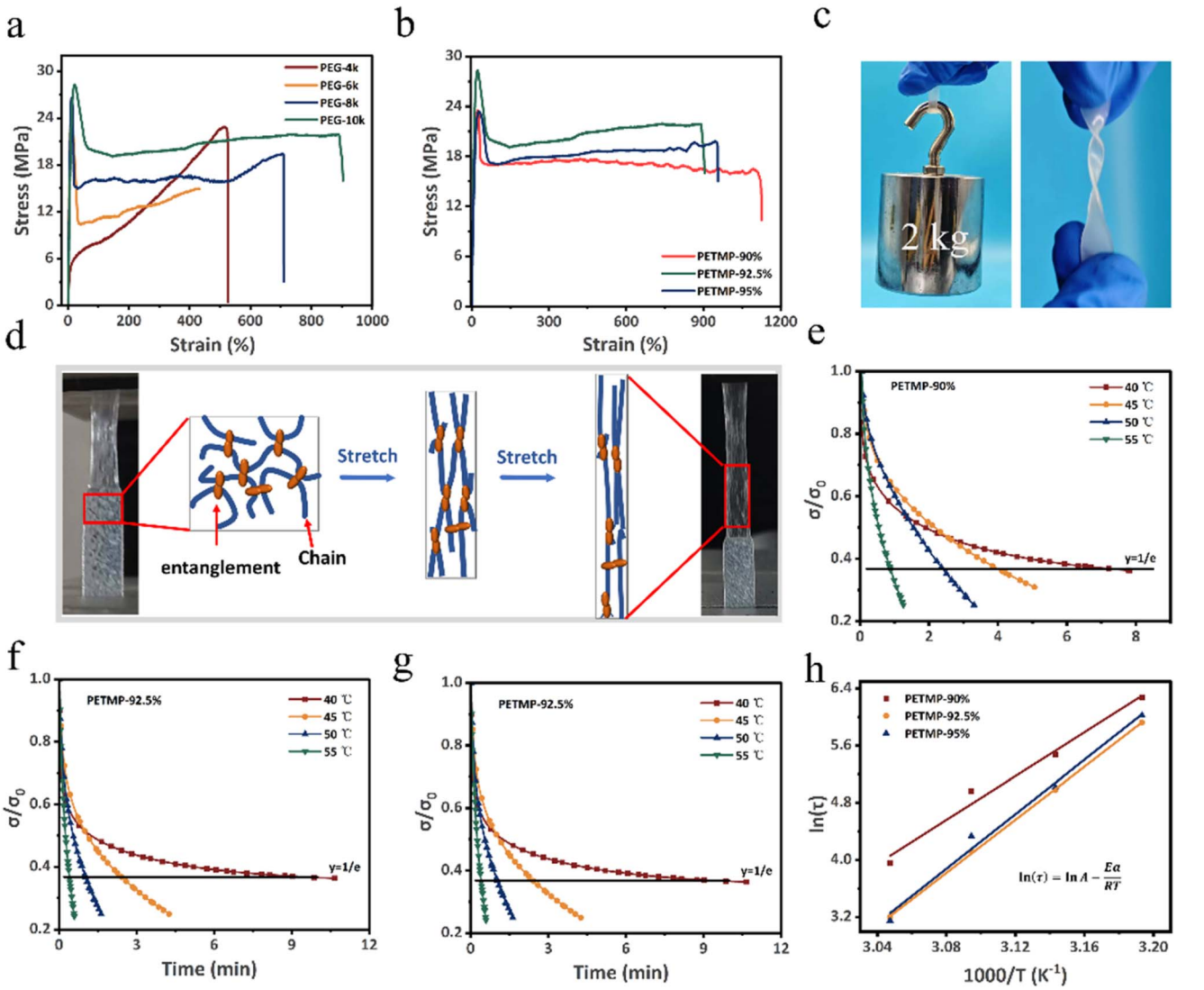

Fig. 3 Mechanical curves with (a) different PEG molecular weights; (b) different PEG-10k contents; (c) digital image of PTUs (40 mg) lifting 2 kg weights and 360° twisting; (d) schematic diagram of superelevation deformation; (e–g) stress relaxation curve; (h) Arrhenius method fitting calculates activation energy of PTUs.

polymer network, which elevates the energy barrier for molecular rearrangement during relaxation. Crucially, the positive dependence of E_a on PETMP concentration directly manifests the role of dynamic covalent bonds in governing stress relaxation kinetics, where heightened TCB density restricts segmental mobility and amplifies temperature sensitivity.

The working principle of the synthesized phase change thermal units (PTUs) is illustrated in Fig. 4a. Upon exposure to ambient temperatures exceeding the melting point of PTUs, the material undergoes a phase transition from its crystalline state to an amorphous state through latent heat absorption, thereby achieving efficient thermal energy storage. Conversely, when ambient temperatures drop below the melting point, the system reversibly transitions back to its crystalline configuration with associated heat release. A critical structural innovation involves the covalent insertion of PEG molecules into the polymer backbone matrix through chemical modification. This architectural design creates a physical constraint that effectively immobilizes the amorphous PEG phase during thermal cycling, thereby eliminating material leakage while maintaining the integrity of the composite structure. The phase change process operates in a closed system, enabling cyclic energy storage and release without compromising the mechanical stability of the polymer matrix.

The thermal phase change properties of the synthesized polyurethane-based phase change materials (PTUs) were evaluated using differential scanning calorimetry (DSC), focusing on the latent heat (ΔH) and phase transition temperature as key indicators of their energy storage and release capabilities. The DSC thermograms of the raw PEG and the fabricated PTUs (Fig. 4b–d) illustrate distinct endothermic and exothermic peaks within the temperature range of 10–60 °C, corresponding to the melting and crystallization processes of PEG segments. These results confirm that the PTUs retain the fundamental

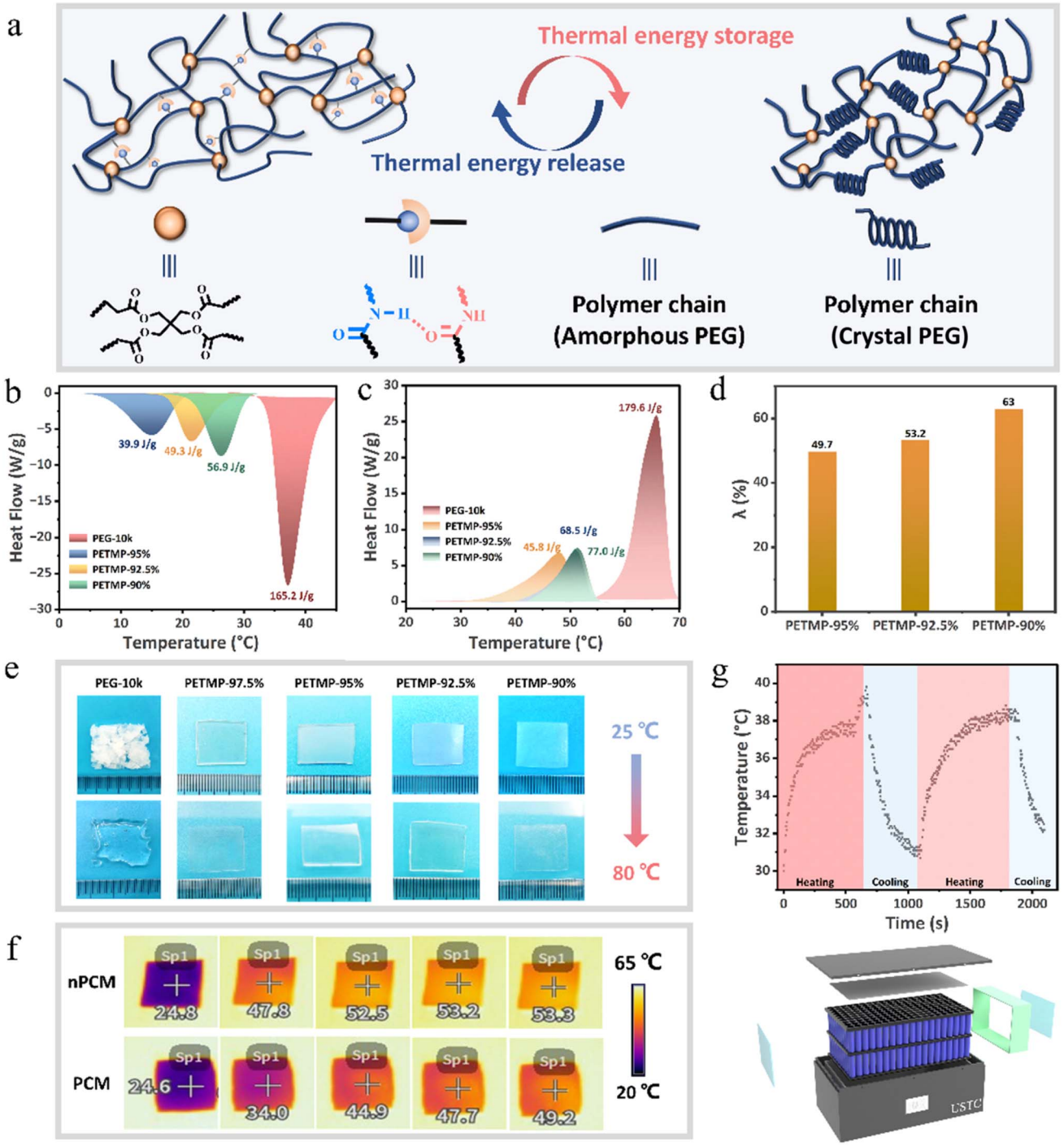

Fig. 4 (a) Schematic illustration of the working mechanism of the PTUs on thermal energy storage/release process, (b–d) DSC, enthalpy change and latent heat efficiency, (e) leak testing, (f) infrared thermal imaging, (g) battery thermal management of PTUs.

phase change behavior of the original PEG, demonstrating their reversible thermal energy storage and release characteristics over a practically relevant temperature range. However, a comparison of the enthalpy values reveals that the phase change enthalpies of the PTUs—represented by PETMP-95%, PETMP-92.5%, and PETMP-90%—are significantly lower than that of pure PEG. Specifically, the measured ΔH values are 45.9, 58.5, and 77.0 J g^{-1} respectively, indicating a progressive increase in latent heat capacity with higher PEG content. This trend suggests that the incorporation of rigid hard segments and the formation of hydrogen-bonded cross-linked networks in the PTUs constrain the mobility and crystallization of the PEG soft segments, thereby reducing their effective phase change capacity. To quantitatively assess the influence of the hard segments on the thermal performance of the PTUs, the latent heat efficiency (λ) was introduced as a performance

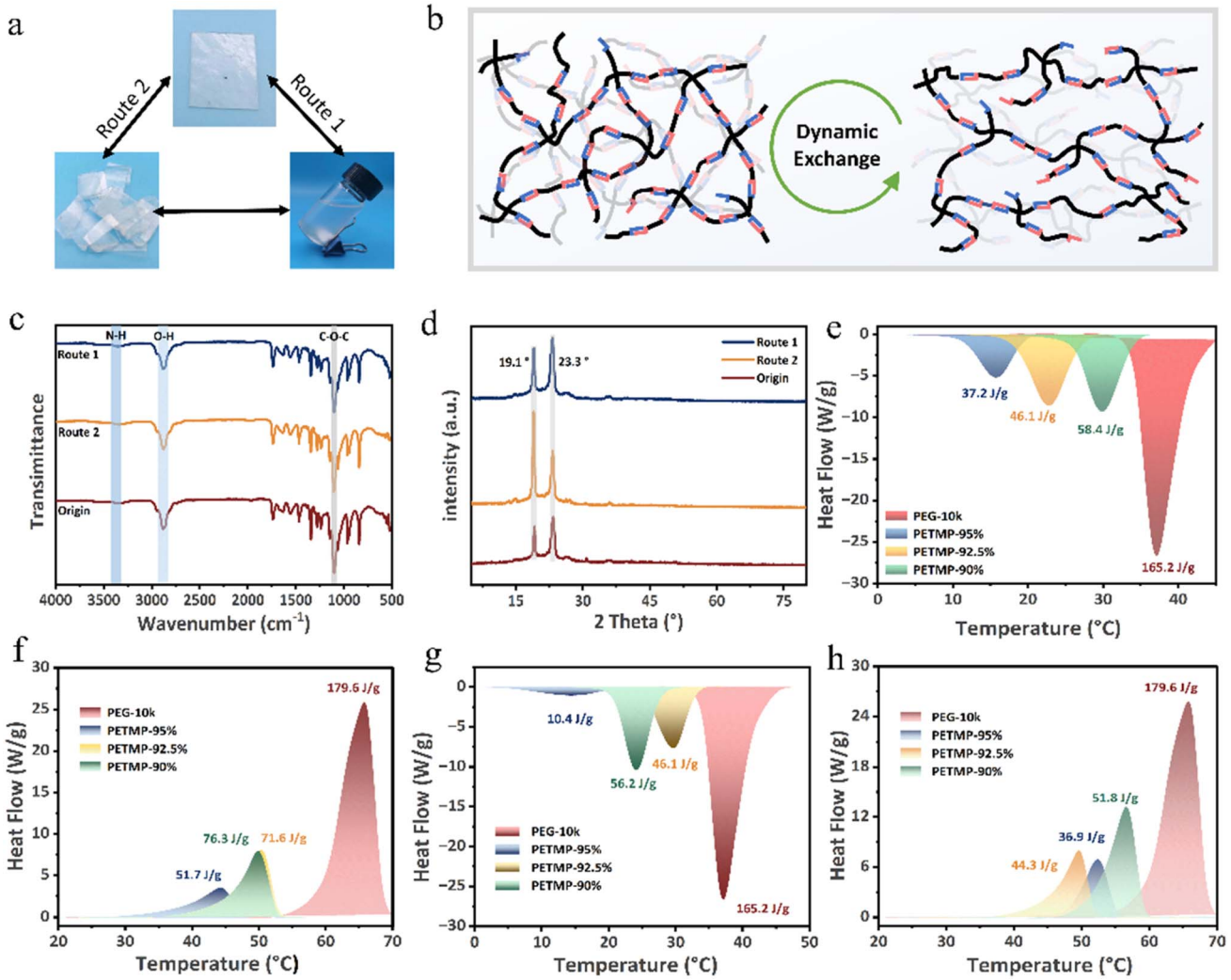

Fig. 5 (a) Recovery route of PTUs. Route 1: dissolution and re-cross-linking. Route 2: hot pressing and re-processing. (b) Schematic illustration of the working mechanism of the PTUs on thermal energy storage/release process. (c) FT-IR. (d) XRD (e and f) DSC and enthalpy change recycled by route 1. (g and h) DSC and enthalpy change recycled by route 2.

metric. The latent heat efficiency is defined as the ratio between the actual phase change enthalpy of the PTU and the theoretical maximum enthalpy based on the PEG content. The calculated λ values—49.7%, 53.2%, and 63.0% for PETMP-95%, PETMP-92.5%, and PETMP-90%, respectively—indicate that the restrictive effect of the hard segments diminishes with increasing PEG concentration. This implies that while the hard segments are essential for structural integrity and shape-stabilization of the composite material, they also interfere with the segmental motion and ordered arrangement of the PEG chains.

In order to verify the solid-solid phase change characteristics of PTUs, a multi-temperature leakage test was carried out systematically. The test results showed that the original PEG was completely melted at the test temperature, while all PTUs samples remained stable in their solid state after 30 min at 80 °C (Fig. 4e). The observation showed that there was no significant deformation or dimensional change of the PTUs material, which was mutually confirmed by the results of previous rheological tests and DMA, which jointly confirmed the morphological stability of the material during the phase transition. This solid-solid transition behavior avoids the risk of liquid phase leakage, highlights the constraint effect of the cross-linked network structure on the PEG chain segment, and provides key performance support for the practical application of the material in thermal energy storage systems.

Fig. 4f and S6 present the temperature–time profiles of heating and cooling processes for PCMs (PETMP-90%) in comparison to non-phase change materials (nPCMs) under constant thermal conditions. It is observed that PCMs display a prolonged near-constant temperature plateau during both heating and cooling phases, indicative of the latent heat absorption and release associated with their phase transition behavior. The overall temperature variation reveals that PCMs exhibit a significantly lower heating rate compared to nPCMs, with the time required to reach thermal equilibrium nearly

doubling from approximately 400 seconds to close to 800 seconds, a phenomenon attributed to the latent heat storage capacity of PCMs during the thermal transition process.

Fig. 4g evaluates the application of PCMs in real-world battery use, while using an infrared (IR) thermal imager to monitor the temperature distribution over time. The use of PCMs significantly extends the time to reach thermal equilibrium and effectively reduces the maximum temperature – PCMs protect cells up to 39.8 °C and bare cells up to 49.4 °C.

In order to evaluate the dynamics of polymer materials, two routes were designed to achieve the dynamic properties of PTUs, one is to use the degradation-relinking process: the PTUs are degraded in DMF at 80 °C, and then placed in the mold to dry and then cross-link to obtain the film, which is called route 1; the second is through the hot pressing–reprocessing process: PTUs can be re-obtained by hot pressing at 130 °C, 10 MPa for 5 min, which is called route 2, as shown in Fig. 5a. With these two recycling routes, the recycling of PTUs can be easily achieved.

Fig. 5b illustrates the dynamic performance of the PTU network, where the reversible transcarbamoylation between TCBs operates as the dominant exchange mechanism. Under thermal or mechanical stimulation, the TCBs undergo rapid bond scission and re-formation, enabling the network topology to rearrange without permanent loss of connectivity. This dynamic equilibrium endows the PTU with autonomous self-repair capabilities: microscopic cracks are spontaneously healed as mobile TCBs segments diffuse across the damage interface and re-establish covalent linkages, restoring mechanical integrity within minutes at elevated temperatures. Concurrently, the same exchange chemistry facilitates efficient reprocessing; the material can be compression-molded or extruded multiple times while maintaining its original tensile strength and modulus, because the continual reshuffling of TCBs erases prior thermo-mechanical history and reconfigures a uniform, defect-free network.

A comparison of the FTIR spectra between the original and the two recycled films revealed nearly identical spectra, indicating that the PTUs maintained the chemical integrity of the material after processing (Fig. 5c).

The XRD spectra before and after recycling are shown in Fig. 5d. It can be observed that there is no significant change in the spectra of route 1 before and after recycling; however, the relative peak intensity of the XRD for PTUs after route 2 recycling changes. This is due to the alteration in the thermal treatment methods for the two, which affects the texture (preferred orientation) of the PTUs material, resulting in a significant enhancement of the (120) phase. The tensile test shows that the strength of the two recycled films and the original material is only slightly reduced, to 22.2 MPa and 19.0 MPa, respectively, with a recovery rate of 94% and 80%, respectively, showing excellent recovery performance of PTUs (Fig. S8).

In order to evaluate the heat storage performance of PTUs before and after recovery, the enthalpy of PTUs in the two recovery routes was tested, and for route 1, the enthalpy size of PTUs before and after recovery was basically maintained (Fig. 5e and f). For route 2, the enthalpy of PTUs decreased before and after recovery (Fig. 5g and h), which is consistent with the phase change indicated by XRD.

Conclusion

In this work, we have developed polythiourethane-based PEG phase change materials for sustainable and structured thermal management materials. The synergistic effect of crosslinking density and dynamic bond makes it have both high strength (28.3 MPa) and high ductility (976.0%), which is far superior to that of traditional brittle PCM materials. Based on the dynamic reversibility of thiocarbamate bonds, two efficient recovery methods were developed, namely solvent-assisted decrosslinking and hot press molding, with a recovery rate of more than 90%. The structural design of the material, such as the nanoscale phase separation domain, not only optimizes the thermal energy storage efficiency, but also achieves self-healing properties similar to biological tissues through its dynamic crosslinking network. Compared with traditional plastics, the material shows great application potential in the fields of electronic product thermal management and building energy conservation, providing a sustainable solution to solve the problem of overheating of electronic devices and reduce plastic pollution. This research opens up a new direction for the development of a new generation of intelligent thermal management materials.

Methods

Materials

Isophorone diisocyanate (IPDI), pentaerythritol tetrakis(3-mercapto-propionate) (PETMP), polyethylene glycol (PEG, M_n = 4k, 6k, 8k, 10k), dibutyltin dilaurate (DBTDL), *N*,*N*-dimethylformamide (DMF) were obtained from China National Pharmaceutical Group Co., Ltd. All the above-mentioned chemical reagents were used without further purification.

Synthesis of PTUs

The reaction process is illustrated in Fig. S1 (SI). The general synthesis procedure is as follows: first, IPDI is weighed and dispersed in a DMF solution. A DMF solution of PEG is then added dropwise to the mixture over a period of 80 min. This step constitutes the pre-polymerization phase. Subsequently, PETMP is weighed, dissolved in a DMF solution, and added dropwise to the prepolymer at 80 °C for 120 min. This step is referred to as chain extension. The resulting extended products are poured into a silicone mold, placed in an 80 °C conventional oven to dry, and finally demolded to obtain the PTU films.

Experimental and characterization apparatus

Details of experimental and characterization apparatus are listed in the SI.

Author contributions

Xiaohua Liu: writing-original draft, data curation, investigation. Hongfei He: writing-reviewing & editing, investigation, validation. Hongliang Ding: conceptualization. Chuanshen Wang: investigation. Lu Liu: investigation. Na Sun: writing-review & editing. Keqing Zhou: validation. Wei Yang: methodology. Jixin Zhu: supervision. Bin Yu: funding acquisition.

Conflicts of interest

The authors declare no conflict of interest.

Data availability

The data supporting this article have been included as part of the supplementary information (SI). Supplementary information is available. See DOI: https://doi.org/10.1039/d5ta10488b.

Acknowledgements

This work was supported by the National Natural Science Foundation of China (No. 22575238, 52321003), the National Key Research and Development Program of China (No. 2021YFB3700202), 100-Young-Talent Program of Chinese Academy of Sciences (KJ2320007002), the National Science Fund for Excellent Young Scholars of China (Overseas, GG2320007003), the Anhui Province Science and Technology Breakthrough Plan Project (No. 202423i08050016), the Experimental Center of Engineering and Materials Sciences from University of Science and Technology of China, and the USTC Center for Micro and Nanoscale Research and Fabrication. This work was partially carried out at the Instruments Center for Physical Science, University of Science and Technology of China.

References

1 Z. Wang, Z. Tong, Q. Ye, *et al.*, Dynamic tuning of optical absorbers for accelerated solar-thermal energy storage, *Nat. Commun.*, 2017, **8**(1), 1478.
2 B. Kalidasan and A. K. Pandey, Next generation phase change materials: state-of-the-art towards sustainable future, *Prog. Mater. Sci.*, 2025, **148**, 101380.
3 A. Usman, F. Xiong, W. Aftab, *et al.*, Emerging solid-to-solid phase-change materials for thermal-energy harvesting, storage, and utilization, *Adv. Mater.*, 2022, **34**(41), 2202457.
4 J. Tao, J. Luan, Y. Liu, *et al.*, Technology development and application prospects of organic-based phase change materials: an overview, *Renewable Sustainable Energy Rev.*, 2022, **159**, 112175.
5 M. R. Anisur, M. H. Mahfuz, M. A. Kibria, *et al.*, Curbing global warming with phase change materials for energy storage, *Renewable Sustainable Energy Rev.*, 2013, **18**, 23–30.
6 H. Zhang, J. Mai, S. Li, *et al.*, Multi-functional phase change materials with anti-liquid leakage, shape memory, switchable optical transparency and thermal energy storage, *Adv. Compos. Hybrid Mater.*, 2022, **5**(3), 2042–2050.
7 C. Baylis and C. A. Cruickshank, Review of bio-based phase change materials as passive thermal storage in buildings, *Renewable Sustainable Energy Rev.*, 2023, **186**, 113690.
8 Y. Zhao, B. Zou, T. Zhang, *et al.*, A comprehensive review of composite phase change material based thermal management system for lithium-ion batteries, *Renewable Sustainable Energy Rev.*, 2022, **167**, 112667.
9 E. Rahimi, A. Babapoor, G. Moradi, *et al.*, Personal cooling garments and phase change materials: a review, *Renew. Sustain. Energy Rev.*, 2024, **190**, 114063.
10 J. S. Cui, W. K. Li, Y. J. Wang, *et al.*, Ultra-stable phase change coatings by self-cross-linkable reactive poly(ethylene glycol) and MWCNTs, *Adv. Funct. Mater.*, 2022, **32**(10), 2108000.
11 J. Qiu, D. Huo and Y. Xia, Phase-change materials for controlled release and related applications, *Adv. Mater.*, 2020, **32**(25), 2000660.
12 C. Yu, J. Park, J. R. Youn, *et al.*, Sustainable solar energy harvesting using phase change material (PCM) embedded pyroelectric system, *Energy Convers. Manage.*, 2022, **253**, 115145.
13 Y. Li, X. Zhao, Y. Tang, *et al.*, Mineral-based composite phase change materials assembled into 3D ordered aerogels for efficient wearable filtration and thermal management, *Adv. Funct. Mater.*, 2024, **34**(39), 2403059.
14 S. Wang, R. Du and T. Li, Progress and perspective on thermal conductivity enhancement of phase change materials, *Sci. Bull.*, 2024, **69**(20), 3176–3179.
15 C. Liu, T. Xiao, J. Zhao, *et al.*, Polymer engineering in phase change thermal storage materials, *Renewable Sustainable Energy Rev.*, 2023, **188**, 113814.
16 Z. Wang, S. Liu, C. Zhu, *et al.*, Physical-entanglements-supported polymeric form stable phase change materials with ultrahigh melting enthalpy, *Adv. Mater.*, 2024, **36**(30), 2403889.
17 X. Jia, Q. Li, C. Ao, *et al.*, High thermal conductive shape-stabilized phase change materials of polyethylene glycol/boron nitride@chitosan composites for thermal energy storage, *Composites, Part A*, 2020, **129**, 105710.
18 S. Li, X. Jiao, L. Chai, *et al.*, Assembling halloysite nanotubes in nickel foam with silica fibers as scaffold for efficiently encapsulating phase change materials towards solar-thermal-electric energy conversion and management, *Chem. Eng. J.*, 2025, **510**, 161681.
19 Z. Liu, Q. Hu, S. Guo, *et al.*, Thermoregulating separators based on phase-change materials for safe lithium-ion batteries, *Adv. Mater.*, 2021, **33**(15), 2008088.
20 M. Xu, C. Shi, P. Li, *et al.*, Thermal expansion challenges and solution strategies for phase change material encapsulation: a comprehensive review, *Adv. Funct. Mater.*, 2024, **34**(51), 2409884.
21 S. Zhang, D. Feng, L. Shi, *et al.*, A review of phase change heat transfer in shape-stabilized phase change materials (ss-PCMs) based on porous supports for thermal energy storage, *Renewable Sustainable Energy Rev.*, 2021, **135**, 110127.

22 J. L. Bento, E. Brown, S. J. Woltornist, *et al.*, Thermal and electrical properties of nanocomposites based on self-assembled pristine graphene, *Adv. Funct. Mater.*, 2017, **27**(1), 1604277.
23 C. Tian, J. Ning, Y. Yang, *et al.*, Super tough and stable solid-solid phase change material based on π-π stacking, *Chem. Eng. J.*, 2022, **429**, 132447.
24 Y. Zhao, T. Liu, Z. Wei, *et al.*, Polymeric phase change material networks based on multi-telechelic polyethylene glycol-derived multimer structures for thermal energy storage, *Chem. Eng. J.*, 2023, **462**, 142164.
25 C. Wang, X. Geng, J. Chen, *et al.*, Multiple H-bonding cross-linked supramolecular solid-solid phase change materials for thermal energy storage and management, *Adv. Mater.*, 2024, **36**(11), 2309723.
26 B. Wu, Y. Wang, Z. Liu, *et al.*, Thermally reliable, recyclable and malleable solid-solid phase-change materials through the classical Diels-Alder reaction for sustainable thermal energy storage, *J. Mater. Chem. A*, 2019, **7**(38), 21802–21811.
27 Y. Wu, M. Chen, G. Zhao, *et al.*, Recyclable solid-solid phase change materials with superior latent heat via reversible anhydride-alcohol crosslinking for efficient thermal storage, *Adv. Mater.*, 2024, **36**(16), 2311717.
28 Y. Huan, M. Gu, Y. Ni, *et al.*, Highly flexible, healable and degradable polyurethane phase change materials with exceptional mechanical properties for thermal regulation, *Chem. Eng. J.*, 2023, **468**, 143742.
29 H. Zhu, M. Gu, X. Dai, *et al.*, Mechanically strong, healable, and recyclable supramolecular solid-solid phase change materials with high thermal conductivity for thermal energy storage, *Chem. Eng. J.*, 2024, **494**, 153235.
30 Z. Wei, Y. Liao, T. Liu, *et al.*, Design of sustainable self-healing phase change materials by dynamic semi-interpenetrating network structure, *Adv. Funct. Mater.*, 2024, **34**(7), 2312019.
31 T. Liu, Y. Zhao, Y. Lei, *et al.*, Catalyst-free, reprocessable, intrinsic photothermal phase change materials networks based on conjugated oxime structure, *Chem. Eng. J.*, 2022, **450**, 138144.
32 H. He, L. Liu, H. Ding, *et al.*, Biomimetic nanostructured polyimine aerogels with graded porosity, flame resistance, intrinsic superhydrophobicity, and closed-loop recovery, *ACS Nano*, 2024, **18**(52), 35465–35479.
33 H. Ding, L. Liu, C. Wang, *et al.*, Highly transparent, mechanically strong, recyclable, and flame-retardant vanillin-modified poly(urethane-urea) elastomers via dynamic oxime-urethane bonds and hydrogen bonds, *Chem. Eng. J.*, 2025, **514**, 163416.
34 R. Wang, Y. Xiao and J. Lei, A solid-solid phase change material based on dynamic ion cross-linking with reprocessability at room temperature, *Chem. Eng. J.*, 2020, **390**, 124586.
35 X. Liu, H. He, H. Ding, *et al.*, Engineering bio-chain extender and DOPO-based flame retardant toward intrinsically flame retardant and mechanically robust polyurea, *Polymer*, 2025, **329**, 128437.
36 X. Lopez De Pariza, P. Fanlo, L. Polo Fonseca, *et al.*, Polythiourethanes: synthesis, applications, and opportunities, *Prog. Polym. Sci.*, 2023, **145**, 101735.
37 C. Cui, L. An, Z. Zhang, *et al.*, Reconfigurable 4D printing of reprocessable and mechanically strong polythiourethane covalent adaptable networks, *Adv. Funct. Mater.*, 2022, **32**(29), 2203720.
38 S. Zhou, F. Tong, M. Chen, *et al.*, Self-evolution of high mechanical strength dry-network polythiourethane thermosets into neat macroscopic hollow structures, *Angew. Chem., Int. Ed.*, 2022, **61**(14), e202117195.
39 X. Zhang, K. Li, C. Wang, *et al.*, Facile and rapid fabrication of a novel 3D-printable, visible light-crosslinkable and bioactive polythiourethane for large-to-massive rotator cuff tendon repair, *Bioact. Mater.*, 2024, **37**, 439–458.
40 K. Wang, T. Zhang, C. Li, *et al.*, Shape-reconfigurable transparent wood based on solid-state plasticity of polythiourethane for smart building materials with tunable light guiding, energy saving, and fire alarm actuating functions, *Composites, Part B*, 2022, **246**, 110260.